JOURNAL OF MATERIALS SCIENCE 31 (1996) 4347–4355

Thixotropic casting of ceramic–metal functionally gradient materials

A. J. RUYS*, J. A. KERDIC, C. C. SORRELL
Department of Ceramic Engineering, School of Materials Science and Engineering, University of New South Wales, Sydney, NSW 2052, Australia

Functionally gradient materials (FGM), a recent development in composite materials, consist of a continuously graded interface between two component phases. Previously reported FGM fabrication methods are reviewed, including vapour deposition, plasma spraying, electrophoretic deposition, controlled powder mixing, slipcasting, sedimentation forming, centrifugal forming, laser cladding, metal infiltration, controlled volatilization, and self propagating high-temperature synthesis. A novel approach to FGM fabrication is presented involving thixotropic casting – vibratory casting of highly concentrated highly thixotropic suspensions castable only under vibration. The hydroxyapatite/316L stainless steel system (a biocompatible ceramic/metal system) was used due to appropriate matches in true densities, thermal expansion, and sintering temperatures. Solids loadings from 76.08–82.67 wt% were trialled. Solids loading was found to be critical. At 78.17 wt%, an ideal continuous FGM formed, showing a gradual transition from pure ceramic to pure metal across 60 mm. At the nearest increments trialled ($\pm$0.3 wt%) gradation was far from optimal: 77.87 wt% gave a sharp ceramic/metal interface with negligible grading; 78.47 wt% gave a relatively homogeneous sample with only a small degree of grading, from a slightly metal-rich end to a slightly metal-poor end.

1. Introduction

Functionally gradient materials (FGMs) are a new class of composite materials characterized by a continuously graded interface between two component phases, most commonly ceramic/metal, although ceramic/ceramic and metal/metal FGMs are also fabricated. The concept originated in Japan in 1984 with the idea of developing a material capable of withstanding severe thermal gradients at high temperatures for applications in the nuclear and aerospace industries. For example, in the aerospace industry, the development of Mach 10 + space planes is dependent on the existence of thermal barrier materials with the capacity to withstand a surface temperature of 2000 K and a temperature gradient of 1000 K across a cross section of 10 mm or less, an application for which FGMs are the only practical solution [1]. While the thermal barrier role of FGMs is predominantly a high-technology application, improvements in ceramic/metal and ceramic/ceramic bonding through the FGM concept have applications in a large number of low- and high-technology applications. This is because FGMs are an ideal solution to the problem of thermomechanical property mismatch at the interface in a ceramic/metal bond, and also in a ceramic/ceramic bond.

In 1987, a national Japanese project was initiated with the purpose of investigating FGM preparation using vapour deposition, plasma spraying, powder metallurgy, and combustion synthesis. By the early 1990s, investigators from other countries also began to publish in the area and, by 1994, Japan accounted for ~60% of published articles with the USA accounting for ~20%. Other significant participants were the UK (<10%) and China (<10%). With this rapid growth in interest in FGM research, a number of FGM fabrication methods have now been documented in the literature. These methods are summarized in Table 1. In general, four approaches to FGM fabrication have been pursued:

1. FGM films (thick and thin).
2. Bulk FGMs – layered.
3. Bulk FGMs – continuous.
4. Component specific methods (for layered or continuous bulk FGMs).

1.1. Fabrication of FGM films

Functionally gradient films represent an ideal solution to thermomechanical property mismatch between the substrate and film material. FGM films are therefore inherently more resistant than conventional films to spalling. Functionally gradient films have been prepared by vapour deposition and plasma spraying. Electrophoretic deposition (EPD) also has been shown to be suitable for this role.

*Author to whom all correspondence should be addressed.

0022–2461

TABLE I Methods reported for FGM fabrication

	FGM type	Fabrication method	References
1	FGM films (Thin and Thick)	Chemical and physical vapour deposition	2–5
		Plasma spraying	6,7
		Electrophoretic deposition	8, 9
2	Layered bulk FGMs	Sequential powder mixtures	10
		Sequential slipcasting	11, 12
		Sequential thixotropic casting	13, 14
3	Continuous bulk FGMs	Controlled powder mixing	15
		Sedimentation forming	16
		Centrifugal forming	17, 18
		Slipcasting	19
		Electrophoretic deposition	8
		Laser cladding	20, 21
		Thixotropic casting	*
4	Component–specific methods for bulk FGMs	Metal infiltration	22, 23
		Controlled volatilization	24
		Self-propagating high-temperature synthesis	25, 26

*This study

1.1.1. Chemical and physical vapour deposition

This involves varying the composition of the depositing gas phase to produce a gradual variation in the composition of the deposited coating to produce FGM thin films. CVD was first used to prepare SiC/C FGM films on graphite substrates using $H_2/SiCl_4/C_3H_8$ gas mixtures [2]. The CVD process also has been used for depositing layered FGM coatings using stepwise variations in the composition of the deposition gas, as in the case of TiC/SiC FGM films from $TiCl_4/SiCl_4/CH_4/H_2$ gas mixtures [3]. As a slight variation on this approach, ZrO_2/Cu FGM films have been fabricated using a combination of CVD and oxygen ion irradiation [4]. PVD also has been used for FGM deposition, for example in the TiC/Ti and TiN/Ti FGM systems [5]. However, vapour deposition techniques suffer from the drawback of slow film-deposition rates.

1.1.2. Plasma spraying

This involves concurrently mixing the two component powders at a gradually varying ratio, in a plasma arc, to produce a graded plasma sprayed coating as a thin or a thick film. This process is considerably quicker than vapour deposition methods. One of the earliest examples of this technique was the low-pressure plasma spraying of ZrO_2/NiCrAlY superalloy FGM coatings producing layered FGM films rather than continuous FGM films [6]. A recent novel application of plasma spraying has been the preparation of functionally gradient diamond films [7].

1.1.3. Electrophoretic deposition (EPD)

EPD can be used to prepare both thin and thick films by deposition of fine particles onto a substrate. This process enables control of deposited layer thicknesses down to ~2 μm with intimately bonded interlaminar interfaces and submicrometre layer smoothness [8]. Although this approach has not yet been used to produce FGM thin films, it has been used to produce alternating microlaminates of Al_2O_3 and ZrO_2 with layer thicknesses as low as 2 μm [9], as well as FGM thick films up to 6 mm thick [8], and so it clearly has the potential of producing a wide range of FGM films.

1.2. Layered (sequential) bulk FGMS

While functionally gradient films have a number of germane applications, bulk FGMs are required in many applications, such as those that involve a structural load-bearing role or a large thermal gradient. These bulk FGMs can be produced as a series of progressive layers, each of fixed composition (layered FGMs), or as a continuous compositional gradient across an interface (continuous FGMs), by a number of methods. Layered FGMs are a distinct improvement over the parent non-FGM two-component composite (pure component *A* bonded to pure component *B*) since the single sharp interface is replaced by a series of "gentle" interfaces between a series of layers of incrementally changing component ratios. However, mismatch still occurs at these layer interfaces, albeit of a reduced intensity. Layered FGMs have been prepared by conventional powder mixing techniques and by sequential slipcasting and sequential thixotropic casting.

1.2.1. Layered powder mixtures

One of the simplest techniques for FGM manufacture is to prepare a layered bulk FGM with each layer consisting of a pre-mixed powder mixture from the two component powders. An example of this was the layered ZrO_2/304 stainless steel FGMs produced by Mihara *et al.* [10], which were produced by conventional powder metallurgy techniques into layers of 100–600 μm thickness varying by 10 vol % increments in the ceramic/metal ratio. The powder metallurgy

approach is however limited in terms of the shape and size of the end product.

1.2.2. Sequential slipcasting

This involves slipcasting a series of layers of differing component ratios to produce a layered FGM. This has been achieved with both ceramic/ceramic FGMs as in the case of Al_2O_3/ZrO_2 [11], and with ceramic/metal FGMs, for example ZrO_2/Ni [12]. Since each layer is of a different particle size distribution (unless the two components have identical particle size distributions), each layer will undergo a different amount of drying shrinkage. These differences in shrinkage between the layers can present problems during the drying stage, although Takebe *et al.* [12] reported that this can be managed by minimizing the differences in permeability and pore radius between the neighbouring layers. Overall, in comparison with layered powder mixing techniques, sequential slipcasting will give much greater flexibility in terms of shape and size of the end product. However production rates are much slower.

1.2.3. Thixotropic casting

Thixotropic casting is a derivative of slipcasting, involving the vibratory casting of highly concentrated highly thixotropic casting slips into porous casting moulds, resulting in a rapid set with minimal shrinkage [13]. The authors have demonstrated the feasibility of sequential thixotropic casting of layered bulk FGMs in the hydroxyapatite/316L stainless steel system, using pre-moistened plaster casting moulds, although the layers with high metal concentrations were difficult to thixotropically cast [14]. This problem was due to the coarse particle size of the metal component, so this therefore could be overcome with the use of finer metal powders. Segregation of the metal and ceramic powders was prevented, by control of the solids loading, enabling the formation of homogeneous layers. Negligible shrinkage occurred in the layers of these sequentially thixotropically cast layered FGMs [14], thereby overcoming the problem of significantly different layer shrinkage rates in sequentially slipcast FGMs [12]. In comparison to the alternatives, thixotropic casting is a much more rapid process than sequential slipcasting, and it offers greater shape and size flexibility than layered powder mixing techniques. However, it has the shortcoming of requiring relatively coarse powders, so reducing the level of densification possible.

1.3. Continuous bulk FGMs

Unlike layered bulk FGMs which contain a number of interfaces between each layer, continuous bulk FGMs consist of an interface-free continuous compositional change from one component to the other. This can occur over a small or a large proportion of the length of the specimen. The larger the length proportion, the more gradual the transition, and hence the less significant is the mismatch problem. Controlled powder mixing methods, gravitational segregation methods, and EPD all have been used to prepare continuous bulk FGMs.

1.3.1. Controlled powder mixing

Although it is theoretically possible to use simple hands-on techniques to prepare dry powder mixtures characterized by a graded composition from one powder to another, this is difficult to achieve reproducibly and economically. Dry powder mixture grading can be achieved by the use of an automated powder spraying and stacking apparatus that progressively varies the component ratio in the sprayed powder mixture [15]. Kawasaki *et al.* [15] have demonstrated the potential of this approach in developing a computer-controlled powder spray stacking apparatus using ethanol slurries. The stacked compacts then are sintered to produce a bulk FGM. Although such an approach to FGM manufacture requires the development of a specialized apparatus, it is well suited to large-scale production.

1.3.2. Sedimentation forming

In a two-component powder system such as that used for the powder-forming of an FGM, the two powders will differ on the basis of their respective true densities and particle size/shape characteristics. Therefore, they both will have different sedimentation rates, which will lead to time-dependent segregation of a powder mixture with the denser powder gravitating toward the bottom of the sedimentation column. This feature has been used to prepare continuous Al_2O_3/NiAl FGMs using an organic liquid as the suspension medium [16]. Mutual deflocculation of the powders required careful selection of suspension media and deflocculants. However, with the right combination, the process gave good control over gradation [16]. A significant difference in true density is desirable since it will greatly accelerate the process. However, if the difference in true density is too great, there will be little or no gradation at the interface.

1.3.3. Centrifugal forming

As a natural progression from sedimentation forming, centrifugal casting enables much faster segregation rates with greater control over segregation, which is advantageous when the two components have similar theoretical densities. Centrifugal casting, as a possible FGM manufacturing process, was first trialled in 1990 using Al_2O_3 and plaster as the components, casting FGMs into a ring configuration [17]. The process has since been used with success in ceramic/metal systems including SiC/Al [18]. This process is very sensitive to differences in component true density, so it would be ideal for FGMs in which there is only a small difference in density; otherwise gradation at the interface will be negligible.

1.3.4. Slipcasting

Since slipcasting involves the time-dependent liquid removal of a mineral slurry, leaving a solid residue

that can be dried and sintered, the process is susceptible to gravity segregation effects if the slurry contains constituents of significantly differing true densities. Slipcasting of continuous bulk FGMs (as distinct from sequential slipcasting of layered FGMs) has been achieved by Chu *et al.* [19] in a system characterized by a very large difference in theoretical density: Al_2O_3/WNiCr, densities 3.99 g cm^{-3} and 19.35 g cm^{-3}, respectively. With careful attention to rheology, this approach also should be suited to FGM systems with a smaller difference in true density.

1.3.5. Electrophoretic deposition (EPD)

A novel EPD technique has been recently developed for the preparation of bulk FGMs involving continuous variation of the deposition slurry [8]. This was achieved in the Al_2O_3/ZrO_2 FGM system, depositing onto a graphite substrate, followed by pressureless sintering in air to densify the FGM and remove the graphite substrate. Deposition began from the ZrO_2 suspension, and a stream of the Al_2O_3 suspension was slowly and continuously injected into the bottom of the EPD bath, with the final deposition being conducted with pure Al_2O_3. Although EPD usually is used to prepare coatings and films, it has proven suitable for the preparation of bulk FGMs since a bulk FGM of thickness ~6 mm was produced [8].

1.3.6. Laser cladding

This involves localized surface heating of a moving substrate (one of the FGM components) using a laser beam, combined with continuous feed of the powder of the other FGM component into the moving laser-heated region. This has been used to produce both layered bulk FGMs (Inconel 625 substrate, SiC–Al powder mixture [20]) and continuous bulk FGMs (Ti substrate, Ti–Al–TiB_2 powder mixture [21]). While laser cladding is a very rapid process, it also requires specialized equipment.

1.4. Component-specific fabrication methods for bulk FGMs

In certain cases, the mutual interaction between the component phases used in bulk FGMs enables the use of specialized component-specific fabrication techniques. Component-specific methods have been used to prepare either layered or continuous bulk FGMs. Techniques reported in this category include metal infiltration of porous ceramics, controlled volatilization, and self-propagating high-temperature synthesis (SHS).

1.4.1. Metal infiltration

Molten metal infiltration of a porous ceramic or metal matrix is a well established fabrication technique for conventional (non-FGM) composite materials in which the component combination is suitable with regard to respective melting points and wetting characteristics [22]. Infiltration was recently used to prepare a metal/metal continuous bulk FGM in the W/Cu system [23]. A tungsten monolith with graded pores was fabricated by stacking tungsten powders in a vertical arrangement with progression from a fine to a coarse particle size. This compact was sintered and then infiltrated with molten copper.

1.4.2. Controlled volatilization

A novel component-specific approach involving controlled volatilization has been used to prepare a MgO/304 stainless steel FGM [24]. This was achieved by subjecting a homogeneous mixture of the metal and ceramic powders to a thermal gradient (temperature range 1300–1400°C) during sintering. This was believed to cause a variation in the MgO volatilization rate along the thermal gradient, resulting in an FGM [24].

1.4.3. Self-propagating high-temperature synthesis (SHS)

This is not actually an FGM formation method but rather an efficient densification method for bulk FGMs that have been powder formed into appropriate green compacts by one of the above methods using components that are suitable for SHS, i.e., mutually explosively reactive. Densification by SHS has proven to be very effective in a number of suitable FGM systems. For example, AlN/Ni FGMs have been prepared by SHS of Al/Ni graded powder mixtures under a N_2 atmosphere [25]. The Al reacted to form AlN, leaving the Ni as the residual metal component. Another approach to SHS densification of FGMs has been a combined process using SHS and hot isostatic pressing [26].

1.5. Thixotropic casting: A new FGM forming technique

Thixotropic casting is an infrequently reported ceramic forming technique that involves formulation of a highly concentrated and highly thixotropic casting slip that is castable only under vibration [27]. Maximization of solids loading is achieved by the use of appropriate trace additions of deflocculant (traces of binder also are added for green strength) to the concentrated slip. This concentrated slip is vibro-poured into vibrating porous casting moulds using techniques similar to those used for vibratory casting of concrete. Vibration is terminated after pouring and the casting sets in a matter of minutes. This is because with such high solids loadings, the moisture content is so low that only a negligible amount of moisture need be lost before the slip adopts the "leather hard" state. The high solids-loadings also result in negligible drying shrinkage. Thixotropic casting therefore is a near-net-shape forming process, with the added benefits of low cost and simplicity. In comparison with alternative ceramic forming processes such as die or isostatic pressing, extrusion, injection moulding, and slipcasting, thixotropic casting is the only method capable of producing large complex ceramic matrix composites

or monolithic ceramics free of stress from binder removal and anisotropy [28].

Although it appears that thixotropic casting has previously been used only for monolithic ceramics [27], this process recently has been used by the authors to prepare fibre-reinforced ceramics [13] and layered bulk ceramic/metal FGMs [14]. The present study involved the adaptation of thixotropic casting to the fabrication of continuous bulk ceramic/metal FGMs, an approach not previously reported. This was achieved through thixotropic casting into non-porous moulds instead of the customary porous moulds.

The use of porous moulds results in the characteristic rapid set, involving movement of the "leather hard" drying front from the surface of the casting through to the core of the casting, over a period of minutes. Experience by the authors has shown that FGMs cast in porous moulds undergo greater segregation at the core than at the surface of the casting, since the core attains the leather hard state significantly later. However, with non-porous moulds, dewatering occurs from the air/sample interface at the top rather than from the mould/casting interface. Therefore, the movement of the "leather hard" drying front is slower and occurs along the axis of segregation rather than perpendicular to it as in the case of the porous mould. Although the level of dewatering required to attain the "leather hard" state is extremely small, the setting rate is relatively slow in a non-porous mould, occurring in a matter of hours, rather than minutes as is the case with porous moulds. However, because setting occurs some time after casting, rather than during casting as occurs with porous plaster moulds, homogeneous segregation can occur across the entire cross-section of the FGM during casting, thereby avoiding coring.

For a given system configuration in which mould geometry, ceramic/metal ratio, and the respective densities of the ceramic and metal components are fixed, it should be possible to control the degree of segregation and hence the sharpness of the ceramic/metal gradient, simply by controlling the solids loading. The higher the solids loading, the more resistance there is to segregation during thixotropic casting. The converse also applies.

Ceramic/metal FGMs were prepared in the hydroxyapatite/316L stainless steel system. This FGM system was chosen on the basis of the potential applications of HAp/metal FGMs as bone replacement materials, with the bicompatible metal providing the strength and toughness, and the hydroxyapatite (chemically similar to bone mineral) providing the bioactive surface capable of forming a chemical bond with bone. An important consideration in sintering bulk ceramic/metal FGMs is that the two components should have similar densification temperatures and that the thermal expansion of the metal should be slightly higher, but not unduly higher, than that of the ceramic. If both these criteria are fulfilled, the FGM can be sintered effectively without causing slumping or decomposition of one component, and during cooling the brittle ceramic phase will be placed in compression. Therefore, stainless steel was chosen over other suitably biocompatible metals due to the appropriate alliance of the respective true densities (moderate difference: HAp $\sim 3.16\,g\,cm^{-3}$; 316L stainless steel $\sim 8.00\,g\,cm^{-3}$), densification temperatures (similar), and thermal expansions (metal slightly higher) of the two FGM components [14]. However, one problem with HAp is its tendency to decompose at elevated temperatures (generally 100 °C or more above the minimum densification temperature [29]) into anhydrous calcium phosphates, which are undesirable since they are much more soluble than HAp *in vitro* [30]. Thus, the decomposition temperature of the HAp must be determined since it represents an upper limit to the sintering temperature of HAp-based FGMs.

2. Materials and methods

2.1. Characterization of the ceramic and metal components

A commercial 316L stainless steel powder (66Fe/17Cr/12Ni/2Mn/2Mo wt % basis: Sintec Ltd., Melbourne, Australia) and a commercial hydroxyapatite (HAp: $Ca_{10}(PO_4)_6(OH)_2$) powder (Plasma Biotal Ltd., Tideswell, UK) were used. These two powders were characterized with respect to particle size distribution by laser diffraction (Mastersizer/E, Malvern Instruments, Malvern, UK). The powders were pelletized in cylindrical dies (HAp dia. 10 mm, 30 MPa pressure; steel dia. 20 mm, 300 MPa pressure), and pellets were densified by pressureless sintering at a range of temperatures under a flowing ambient overpressure argon atmosphere using a controlled-atmosphere SiC resistance tube furnace. Sintering curves were then generated for each component from the temperature-density data. Thermal expansion behaviour was measured from 300–1100 °C under a flowing ambient overpressure argon atmosphere using a controlled-atmosphere dilatometer (Dilatometer model 1600, Orton, Westerville Ohio, USA). The decomposition temperature of the HAp was determined by X-ray diffraction (D5000, Siemens, Munich, Germany) of the sintered HAp pellets and corresponded to the temperature at which anhydrous calcium phosphate phases were first detected.

2.2. Thixotropic casting of the FGMs

All FGM trials were conducted using a standardized ceramic: metal ratio of 2 : 1 (volume basis). The higher ceramic content was chosen since the particle size of the metal was an order of magnitude coarser and so the ceramic particles tended to fill the metal pore network. Therefore, for a ceramic content much below 2 : 1, a pure ceramic region did not occur at the top of the FGM. Commercial grades of stainless steel powder metallurgy powders are generally produced with an average particle size in the order of tens of micrometres by atomization. Ultrafine stainless steel powders generally are not commercially available, and conventional milling usually cannot reduce the particle size of the coarse ductile atomized particles below a few tens of micrometres due to the flattening/flaking/welding

equilibrium characteristic of milled ductile powders. Milling at temperatures well below 0°C, sufficiently cold to embrittle the metal, can overcome this limitation. However, this is a costly and complex procedure.

Thixotropic casting slips were formulated using sodium carboxymethylcellulose (Na–cmc) as the sole additive in the dual role of deflocculant and binder, a role to which it is well suited [31]. Optimal deflocculant addition was determined by torsional viscometry (11940/1 torsional viscometer, Gallenkamp Ltd., UK) at the moderate solids loading of ~60 wt % in accordance with previous work by the authors [13]. The Na–cmc was added as a colloidal sol in demineralized water, with the Na–cmc concentration in the sol tailored to produce the desired Na–cmc addition for a given solids loading.

Thixotropic casting slips were formulated by the following steps:

1. Batching of the ceramic and metal powders into perspex vibro-mixing jars at a 2:1 ceramic: metal volumetric ratio.
2. Addition of water and Na–cmc as a Na–cmc sol (by pipette). A total of 11 different solids loadings were trialled: 76.08, 77.31, 77.87, 78.17, 78.47, 78.87, 79.04, 79.60, 80.02, 80.88, and 82.67 wt %.
3. Vibro-mixing in a vibratory mixing mill until the slip reached an equilibrium consistency – generally from 15 min to 120 min (higher solids loadings required longer mixing times).

The low drying shrinkage of the thixotropically cast FGMs (generally $< 1\%$) made mould selection somewhat problematic. With conventional porous moulds, a split configuration is used to enable piecewise removal after casting. However, with the use of non-porous casting moulds, a segmented mould is undesirable due to the air-gaps between the segments. To solve this problem, three types of mould configuration were trialled. In each case the mould cavity was cylindrical with a standard height of 60 mm. The three mould configurations, were as follows:

1. Wax mould cavity, removable by melting (diameter 15 mm).
2. Glass tube with impermeable removable base (inside diameter 17 mm).
3. Glass tube with impermeable removable base (as above), but with a removable plastic sheath inside the mould to isolate the casting from the mould to facilitate removal of the casting.

2.3. Characterization of the FGMs

After casting, the samples were air dried in the moulds in an upright position for one week. They then were removed from the moulds and air dried for a further 2 days, followed by 12 h at 110 °C in a drying oven. The samples then were densified by pressureless sintering at 1350 °C for 1 h at a heating and cooling rate of 100 °C h^{-1}, under a flowing ambient overpressure argon atmosphere. The maximum possible sintering temperature was 1350 °C since it was found that decomposition of the HAp commenced above this temperature.

The sintered FGM samples were set in resin, ground down to reveal the complete longitudinal cross-section, then polished. The bars that appeared to be functionally gradient were then characterized with respect to their compositional profile by scanning electron microscopy (SEM: JXA–840, Jeol Ltd., Tokyo, Japan) and energy dispersive spectroscopy (EDS: AN10000 X-Ray analyser, Link Systems Inc., Bucks, England), scanning for four elements – Ca, P, Fe, and Cr. These four elements corresponded to the dominant two elements of each FGM component, viz., HAp (Ca and P) and 316L stainless steel (Fe, Cr). Further, the uniformity of densification was assessed by making diametral shrinkage measurements along the profile of the FGM, using vernier callipers.

3. Results and discussion

3.1. Thermal expansion

The dilatometry curves, shown in Fig. 1, revealed that the stainless steel had an average thermal expansion of 17.5×10^{-6} cm cm^{-1} K^{-1} while the HAp had an average of 13.5×10^{-6} cm cm^{-1} K^{-1}. In accordance with the criterion that the thermal expansion of the metal should be slightly higher, but not unduly higher, than that of the ceramic, these respective expansion coefficients were quite suitable for an FGM application.

3.2. Densification

The individual pressureless-sintered densification curves for the HAp and the stainless steel are shown in Fig. 2. The X-ray diffraction analysis showed that decomposition of the HAp to anhydrous calcium phosphates began above 1350 °C. Therefore, 1350 °C represented an upper limit for the sintering temperature in this system, at which temperature Fig. 2 reveals that the densification of the stainless steel and the HAp was incomplete, although densification of the HAp was greater at this temperature. The effects of this on the FGM can be seen in the shrinkage versus length data for an optimal FGM, plotted in Fig. 3, and in the slight tapering of the optimal FGM shown in Fig. 4. Densification was greatest at the HAp-rich end, which was consistent with the data presented in Fig. 2. While the focus of the present work was the FGM formation method rather than the densification of the FGM, it is worth noting that the degree of densification at 1350 °C, and the consistency of densification along the length of the FGM, would be much improved through the use of controlled-atmosphere hot-pressing or encapsulated hot-isostatic-pressing.

3.3. Thixotropic casting of the FGMs

The thixotropically cast FGMs, spanning solids loadings from 76.08 to 82.67, exhibited a broad range of casting behaviour. The highest solids loadings were barely pourable under vibration and set much more rapidly than the casting slips with lower solids loadings. The lowest solids loadings resulted in casting slips that did not need vibration when casting into the

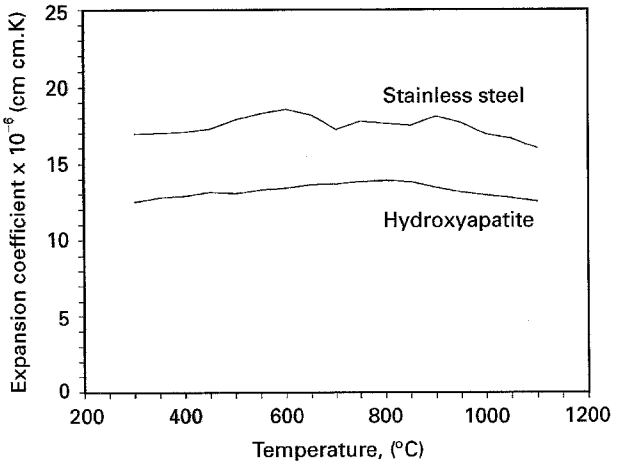

Figure 1 Thermal expansion coefficient (10^{-6} cm cm^{-1} K^{-1}) as a function of temperature for the ceramic (hydroxyapatite) and metal (316L stainless steel) components of the FGM.

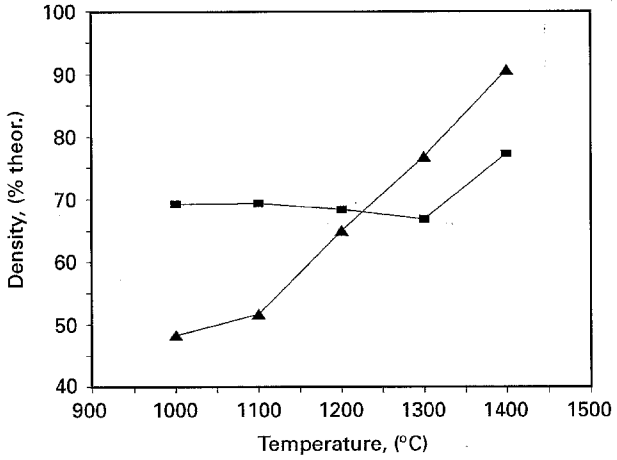

Figure 2 Pressureless sintering curves for; (▲) the ceramic (hydroxyapatite) and (■) the metal (316L stainless steel) components of the FGM.

simple smooth-walled cylindrical non-porous moulds used. However, with the use of more complex moulds, vibration would be advantageous for effective mould filling with such casting slips.

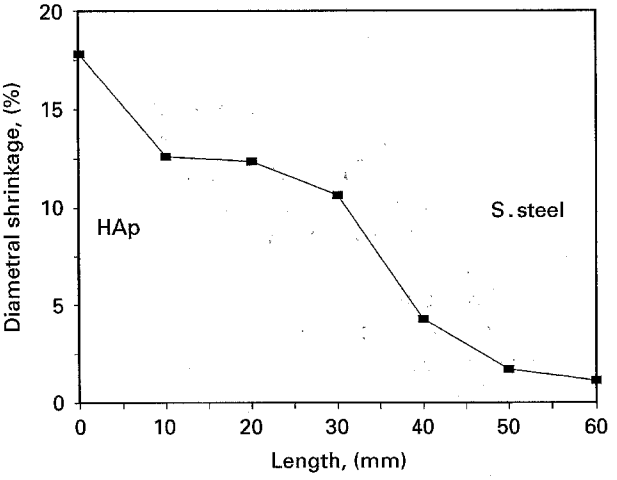

Figure 3 Diametral shrinkage of the optimal FGM (78.17 wt % solids), moving from the ceramic end (hydroxyapatite) to the metal end (316L stainless steel) along the 60 mm length.

The cast FGMS were easily classified by visual inspection into one of three categories:

1. Solids loading > 78.17 wt %: homogeneous or nearly homogeneous – little segregation occurred.
2. Solids loading $= 78.17$ wt %: functionally gradient – a clear gradual graded region between the ceramic and metal regions.
3. Solids loading < 78.17 wt %: sharp interface – little or no gradation between the ceramic and metal regions.

Thus, the optimum solids loading was a very critical parameter, and this will vary, for a given FGM, with each variation in particle size, as previous work has shown [13]. While a continuous gradient was produced at a loading of 78.17 wt %, the nearest adjacent loadings trialled (± 0.3 wt %: i.e., 77.87 and 78.47 wt %) were far from optimal. At 77.87 wt %, segregation was excessive, resulting in a sharp ceramic – metal interface with little or no detectable graded region. At 78.47 wt %, the casting was virtually homogeneous with only a slightly higher metal concentration at the base.

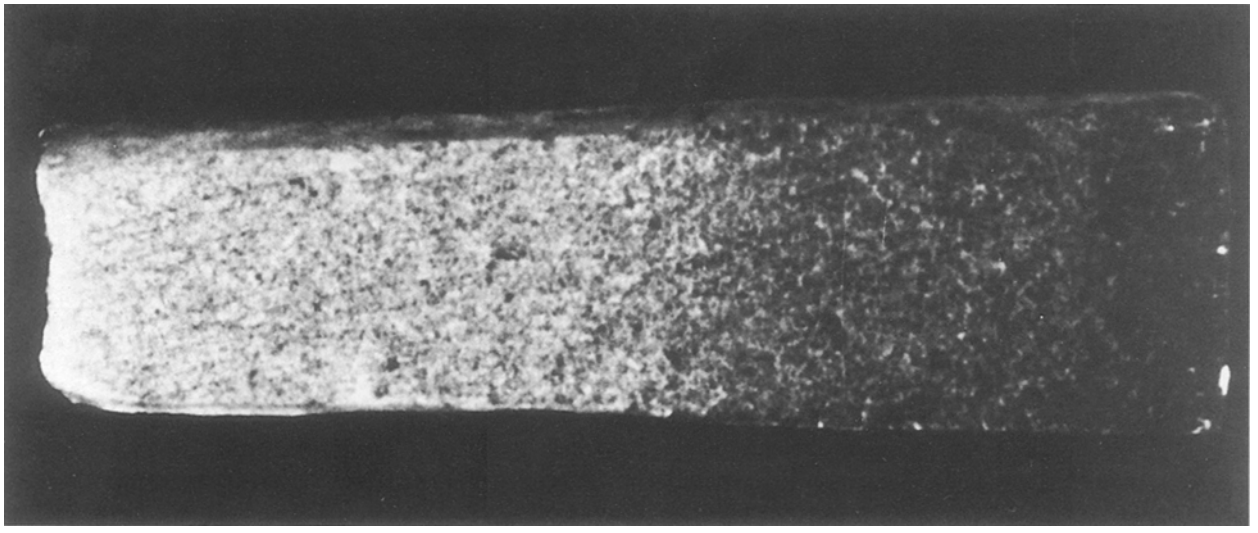

Figure 4 The optimal FGM (78.17 wt % solids), showing a gradual transition from the ceramic end (hydroxyapatite) to the metal end (316L stainless steel) along the 60 mm length.

Fig. 4 shows a longitudinal cross-section of the FGM cast with the optimal solids loading of 78.17 wt %. The sample shows a large gently graded region with a gradual transition from pure ceramic to pure metal across 60 mm – an optimal result for a continuous bulk FGM. Therefore, with careful attention to solids loading, it can be seen that the thixotropic casting process is well suited to the preparation of ceramic-metal FGMs.

An EDS compositional profile of this optimal FGM is shown in Fig. 5 revealing that the stainless steel concentration (Fe, Cr) varied linearly from the HAp-rich top of the casting FGM column (0 mm) to the steel-rich bottom of the casting FGM column (60 mm). The HAp concentration did not vary linearly, but rather, most of the decrease occurred in the last 30% of the length. While these EDS data are only semi-quantitative in nature, this non-linearity in the Ca and P traces appears to be significant. It was probably a result of particle packing phenomena, due to the large difference in particle size between the ceramic and metal components of this FGM system, together with the fact that the HAp concentration in the FGM was twice that of the steel concentration.

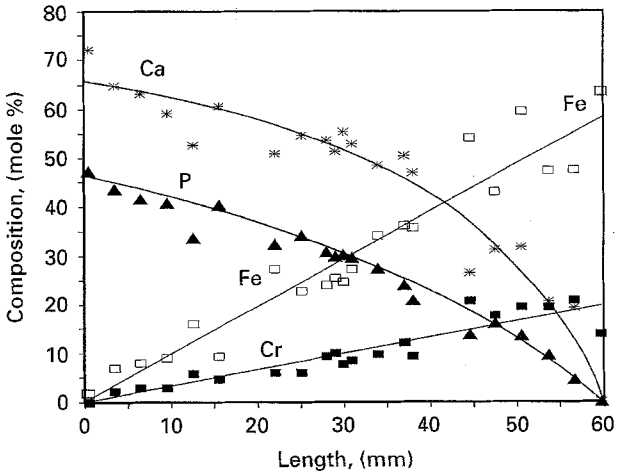

Figure 5 EDS compositional profile of the optimal FGM (78.17 wt % solids), from the ceramic end (hydroxyapatite: Ca, P) to the metal end (316L stainless steel: Fe,Cr) along the 60 mm length.

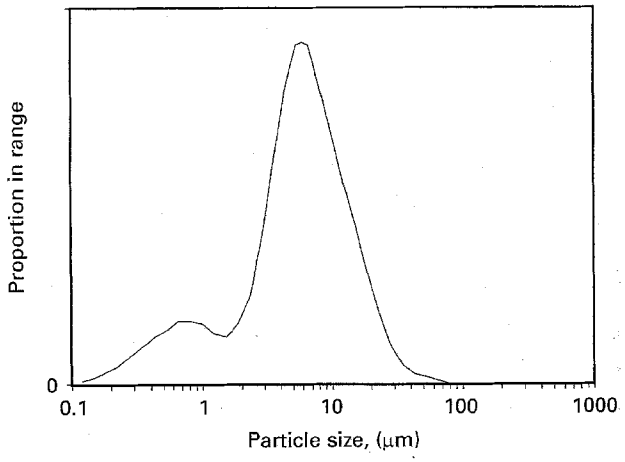

Figure 6 Particle size distribution of the ceramic powder (hydroxyapatite).

Since the HAp particles were very much smaller than the steel particles, and present in much greater quantity, it is logical that the HAp concentration would be higher than the steel concentration from the top of the column until well past the midpoint, as the data in Fig. 5 suggest.

The particle size distributions of the HAp and stainless steel powders are shown in Figs 6 and 7 respectively. Fig. 6 reveals that the HAp had a bimodal distribution with the majority of the particles within the range 2–20 μm, with a small but significant peak in the range 0.2–2 μm. This is because precalcined HAp

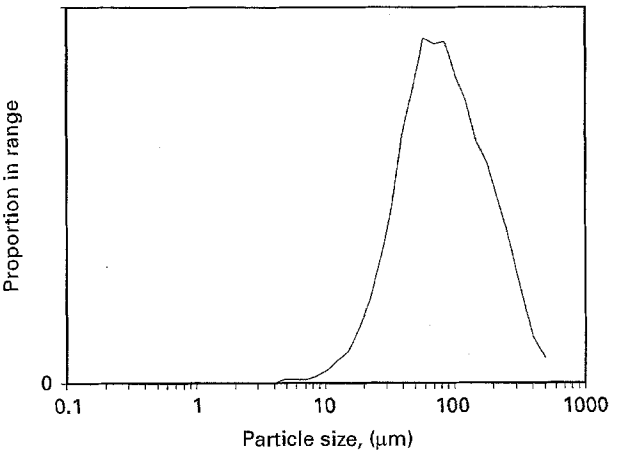

Figure 7 Particle size distribution of the metal powder (316L stainless steel).

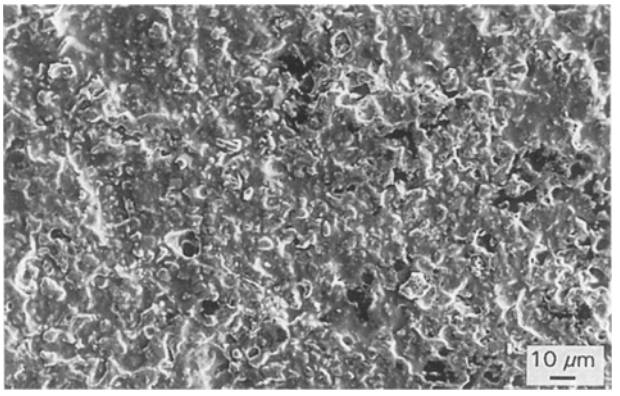

Figure 8 Microstructure of the ceramic (hydroxyapatite) end of the optimal FGM (78.17 wt % solids).

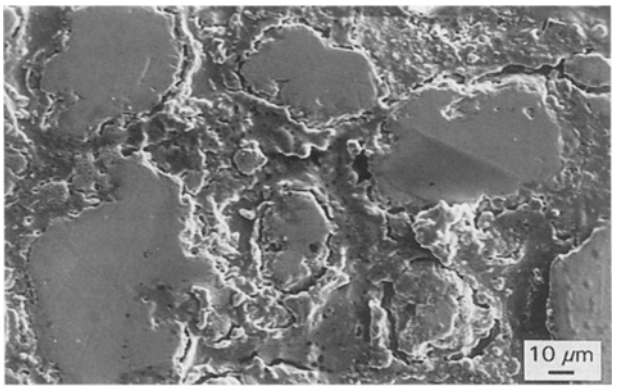

Figure 9 Microstructure of the metal (316L stainless steel) end of the optimal FGM (78.17 wt % solids).

powders consist of agglomerates (micrometre scale) of the nanoparticles produced by chemical precipitation, a phenomenon previously described by Ruys *et al.* [32]. Fig. 7 reveals that the stainless steel powder had a broad particle size distribution with the majority of particles falling within the range 20–500 μm, with an average particle size of 62 μm. This is typical for an atomized steel powder [33].

Thus the majority of particles in this HAp powder were micrometre agglomerates, and a small proportion were nanometre agglomerates and unagglomerated nanoparticles. Comparison of Figs 6 and 7 demonstrates that there was virtually no overlap in the respective size distributions of the HAp and stainless steel powders, with essentially all the stainless steel particles being larger than the HAp particles. The laser diffractometer internal algorithm calculated the average particle size of the HAp powder to be 4.2 μm and that of the stainless steel to be 62 μm. Therefore, on average, the metal particles were ~15 times larger than the ceramic particles.

Figs 8 and 9 demonstrate the effect of the large difference in the particle size of the ceramic and metal components on the microstructure of the resultant FGM. The microstructure at the top of the column (Fig. 8) appears to consist of purely microporous fine-grained HAp, consistent with the EDS scan in Fig. 5 which indicated a composition of predominantly HAp with traces of stainless steel. The microstructure at the base of the column (Fig. 9) consisted of large steel particles surrounded by a matrix. The appearance of the matrix suggests that significant liquid formation occurred. The EDS scan indicated negligible HAp at this point so the liquid was probably due to an interaction between the finer metal particles and the traces of HAp.

4. Conclusions

Thixotropic casting was successfully used to prepare a well-graded continuous bulk ceramic/metal FGM in the hydroxyapatite/316L stainless steel (HAp) system, a system with biomedical applications.

The relative true densities and thermal expansions of the HAp and 316L stainless steel components were well suited to the manufacture of FGMs. The decomposition temperature of the HAp (above 1350 °C) was too low for effective pressureless sintering, indicating the need for subsequent hot pressing or hot isostatic pressing.

Solids loading was critical. At 78.17 wt % solids, an ideal continuous FGM formed showing a gradual transition from pure ceramic to pure metal across 60 mm. A decrease of only 0.3 wt % gave a sharp ceramic/metal interface with negligible grading, and an increase of only 0.3 wt % gave a relatively homogeneous sample with a higher metal concentration at the base than at the top.

References

1. M. NIINO, *J. Jpn. Soc. Powd. Metall.* **37** (1990) 241.
2. M. SASAKI, Y. WANG, T. HIRANO and T. HIRAI, *J. Jpn. Ceram. Soc.* **97** (1989) 539.
3. C. KAWAI, J. TERAKI, T. HIRANO and T. NOMURA, *Ibid.* **100** (1992) 1117.
4. S. NAKASHIMA, H. ARIKAWA, M. CHIGASAKI and Y. KOJIMA, *Surf. Coat. Tech.* **66** (1994) 330.
5. T. HIRAI and M. SASAKI *JSME Int. J. Series I* **34** (1991) 123.
6. T. HASHIDA, H. TAKAHASHI and K. MIYAWAKI, *J. Jpn. Soc. Powd. Metall.* **37** (1990) 307.
7. K. KURIHARA, K. SASAKI, M. KAWARADA and Y. GOTO, *Thin Solid Films* **212** (1992) 164.
8. P. SARKAR, X. HUANG and P. S. NICHOLSON, *J. Amer. Ceram. Soc.* **76** (1993) 1055.
9. *Idem. Ibid.* **75** (1992) 2907.
10. T. MIHARA, T. SATO, Y. KITAMURA and K. DATE, in IEEE 1993 Ultrasonics Symposium Proceedings. Vol. 1. Edited by M. Levy and B.R. McAvoy (IEEE, NY, 1993) p. 617.
11. J. S. MOYA, A. J. SANCHEZ-HERENCIA, J. REQUENA and R. MORENO, *Mater. Lett.* **14** (1992) 333.
12. H. TAKEBE, T. TESHIMA, M. NAKASHIMA and K. MORINAGA, *J. Jpn. Ceram. Soc.* **100** (1992) 387.
13. A. J. RUYS, S. A. SIMPSON and C. C. SORRELL, *J. Mater. Sci. Lett.* **13** (1994) 1323.
14. J. KERDIC, A. J. RUYS and C. C. SORRELL, *Int. Ceram. Monogr.* **1** (1994) 215.
15. A. KAWASAKI, H. HIROSE, H. HASHIMOTO and R. WATANABE, *J. Jpn. Soc. Powd. Metall.* **37** (1990) 922.
16. D. P. MILLER, J. J. LANNUTTI and R. D. NOEBE, *J. Mater. Res.* **8** (1993) 2004.
17. Y. FUKUI, *Nippon Kikai Gakkai Ronbunshu Part C* **56** (1990) 67.
18. Y. FUKUI, Y. OYA-SEIMIYA and K. NAKANISHI *Nippon Kikai Gakkai Ronbunshu, Part A* **57** (1991) 1790.
19. J. CHU, H. ISHIBASHI, K. HAYASHI, H. TAKEBE and K. MORINAGA, *J. Jpn. Ceram. Soc.* **101** (1993) 841.
20. K. M. JASIM, R. D. RAWLINGS and D. R. F. WEST, *J. Mater. Sci.* **28** (1993) 2820.
21. J. H. ABBOUD, D. R. F. WEST and R. D. RAWLINGS, *J. Mater. Sci.* **29** (1994) 3393.
22. S.-Y. OH, J. A. CORNIE and K. C. RUSSELL, *Ceram. Eng. Sci. Proc.* **8** (1987) 912.
23. M. TAKAHASHI, Y. ITOH and M. MIYAZAKI, *Yosetsu Gakkai Ronbunshu* **12** (1994) 289.
24. T. NISHIDA, H. FUJIOKA and T. NISHIKAWA, *J. Jpn. Soc. Powd. Metall.* **37** (1990) 259.
25. K. ATARASHIYA and M. UDA, in Proceedings of the International Conference on Advanced Composite Materials 1993. (Minerals, Metals & Materials Soc, Warrendale, PA, USA, 1993) p. 1351.
26. Y. MATSUZAKI, J. FUJIOKA, S. MINAKATA and Y. MIYAMOTO, *J. Jpn. Soc. Powd. Metall.* **37** (1990) 937.
27. A. J. RUYS and C. C. SORRELL, in Ceramics: Adding the Value, Volume 1, edited by M. J. Bannister (CSIRO, Melbourne, 1992) p. 581.
28. N. EHSANI, A. J. RUYS and C. C. SORRELL, Pacim II: Proceedings of the Second Intl. Symposium of Pacic Rim Ceramic Societies, (in press).
29. A. J. RUYS, M. WEI, C. C. SORRELL, M. R. DICKSON, A. BRANDWOOD and B. K. MILTHORPE, *Biomater.* **16** (1995) 409.
30. P. DUCHEYNE, S. RADIN, M. HEUGHEBAERT and J. C. HEUGHEBAERT, *Ibid.* **11** (1990) 244.
31. A. J. RUYS and C. C. SORRELL, *Bull. Amer. Ceram. Soc.* **69** (1990) 828.
32. A. J. RUYS, C. C. SORRELL, A. BRANDWOOD and B. K. MILTHORPE, *J. Mater. Sci. Lett.* **14** (1995) 744.
33. Metals Handbook. 9th Edition. Volume 7. Powder Metallurgy" (ASM, Metals Park, Ohio, 1984).

Received 12 May 1995
and accepted 1 December 1995